Theoretical investigation on the scale factor of a triple ring cavity to be used in frequency sensitive resonant gyroscopes

C. Ciminelli c.ciminelli@poliba.it Optoelectronics Laboratory, Politecnico di Bari, Via Orabona 4, 70125 Bari, Italy

C. E. Campanella Optoelectronics Laboratory, Politecnico di Bari, Via Orabona 4, 70125 Bari, Italy

F. Dell'Olio Optoelectronics Laboratory, Politecnico di Bari, Via Orabona 4, 70125 Bari, Italy

C. M. Campanella Optoelectronics Laboratory, Politecnico di Bari, Via Orabona 4, 70125 Bari, Italy

M. N. Armenise Optoelectronics Laboratory, Politecnico di Bari, Via Orabona 4, 70125 Bari, Italy

In this paper we study a multi-ring resonant structure including three evanescently coupled ring resonators (named triple ring resonator, TRR), with different ring radii and coupling coefficients, and coupled to two bus waveguides. The potential application of a TRR as a rotation sensor is analyzed and its advantages over a single ring resonator (SRR) under rotation conditions are also highlighted. When the coupled rings have different size and their inter-ring coupling coefficients are lower than the ring-bus coupling coefficients, the resonance frequency difference between two counter-propagating beams induced by rotation is enhanced with respect to that of a single ring resonator (SRR) with the same footprint. The scale factor of the rotating TRR, which depends on the structural parameters (i.e. inter-ring and ring-bus coupling coefficients, lengths of the rings, overall propagation loss within the rings), is up to 1.88 times the value of the scale factor of a SRR, which depends only on the ring radius, by assuming that the waveguide structure in both configurations is the same. This promising numerical achievement results in a reduction of the sensor footprint of about two times, with respect to a single ring with the same scale factor. The results obtained may be useful to define new configurations of frequency sensitive optical gyros in low-loss technology, having a small volume. In fact, by properly choosing the structural parameters, the spectral response of the TRR is forced to assume a shape more sensitive to the resonant frequency shift due to the rotation with respect to that one of a SRR.
[DOI: http://dx.doi.org/10.2971/jeos.2013.13050]

Keywords: Integrated optics, ring resonators, coupled ring resonators, optical gyroscope

1 INTRODUCTION

The wide range of application domains for ring resonators, e.g., space, telecommunications and sensing, makes these devices a very interesting research topic. The physical behavior of both single-ring and multi-ring optical cavities under rotation allows their application in the field of gyroscope systems [1, 2].

Optical gyroscopes based on the Sagnac effect can be active sensors, such as the ring laser gyroscope (RLG), and passive ones, such as the resonant fiber optic gyroscope (RFOG) and the interferometric fiber optic gyroscope (IFOG). Both categories operate by exploiting the rotation induced phase or frequency shift generated between two counter-propagating optical beams. In the RLG, the Sagnac effect occurs in an active optical cavity, able to generate counter-propagating optical beams, while both the IFOG and the RFOG are externally excited by an optical source and require long open optical paths and large size optical resonators, respectively, to detect a measurable phase or frequency shift.

In IFOGs the phase shift between the two counter-propagating beams is detected through an interferometric phase sensitive technique. This technique is based on the detection of a power variation deriving from the interference between two counter propagating beams, which experience a rotation induced phase difference. When the frequency shift has to be detected, a frequency sensitive read-out technique is required, which consists of a spectrometric approach based on the measure of the difference between the resonant frequencies of the two counter-propagating beams.

Several research groups have attempted to exploit integrated optics advantages to produce miniaturized, compact, reliable, and low-cost optical gyroscopes based on either semiconductor ring lasers [3]–[7] or passive ring resonators [8]–[11]. The most encouraging results (with a resolution of a few hundred°/h) have been achieved by resonant micro optical gyros (RMOGs) based on silica waveguiding single-ring [12] or spiral cavities [13, 14] having a footprint less than 10 cm^2 or 20 cm^2.

In the last five years, researchers have paid attention to the

Received February 26, 2013; revised ms. received June 19, 2013; published July 26, 2013 ISSN 1990-2573

development of new angular velocity sensors based on multi-ring structures. The most significant example of these devices is the CROW (coupled-resonator optical waveguide) gyro [15, 16], which is a phase sensitive sensor having an operating principle similar to that of the IFOG. CROW is an optical structure used as delay line for manipulating group velocity of optical pulses in order to obtain a slow light regime. In the CROW, propagation is due to the evanescent coupling between high Q factor micro-cavities, formed by waveguiding rings or photonic crystal defects. Although has been proved [15] the possibility of exploiting the dependence of Sagnac phase shift on the group index in a CROW optical gyro, however the slow light gyros are not suitable for enhancing the Sagnac phase shift of the sensor [16].

Another physical phenomenon, which consists in exploiting the variation of the power transmitted at the central wavelength of the pass band of a loss-less CROW, for detecting an angular velocity change, has been proposed in [17]. Spectral response at rest is characterized by a wide pass band, due to the overall splitting effect, between the resonance wavelengths, due to the coupling of degenerate optical cavities (i.e. ideal cavities with the same resonance wavelength). An issue for this device is that it needs to be rotated at an angular velocity $> 10^{13\circ}/\mathrm{h}$ [17] to be able of detecting the power variation at the central wavelength of the pass band. Moreover, a rotation of that device with an angular velocity $> 10^{13\circ}/\mathrm{h}$ is responsible of the formation of a stop band within the pass band. In fact, the transmission curve at the central wavelength decreases as exp(N), with N the number of the coupled cavities, thus forming the stop band.

By removing the hypothesis of an ideal loss-less CROW gyro, in Ref. [18] Authors demonstrated that the rotation-induced gap in the center of the transmission function is reduced compared to that of a lossless CROW. Propagation losses in a CROW structure are responsible of a region insensitive to rotation at low rotation rates. To overcome this problem, Authors proposed to periodically modulate the resonant frequencies.

Recently, in Ref. [19] a uniform CROW is compared with a CROW formed by non-degenerate micro-ring resonators having radii slightly different each other in order to be called to satisfy a specific chirping law. Coupled chirped area ring resonators resonate at different resonance wavelengths allowing the formation of narrow resonant peaks, instead of a pass band. The narrowest resonance peaks are those closest to the edges of the conventional uniform CROW pass band. This solution allows to scale the number of coupled ring resonators from 35 to 5, to achieve the same transmittance change, due to the rotation, in a uniform CROW. This effect still requires large rotation rates (of about $10^{13\circ}/\mathrm{h}$) to be appreciated with the same phase sensitive read-out technique of a conventional CROW. Same Authors in [20] extended the idea of a 'chirped area' CROW to a CROW configuration having variable coupling coefficients. In particular, they theoretically demonstrated that a periodic modulation of the evanescent coupling between ring resonators can lead to a sharp transmission resonance instead of a wide pass band. They claim that, through this principle, a phase sensitive interferometric gyroscope having a resolution of $0.002^\circ/\mathrm{h}$ and occupying a micrometric area of 0.16 mm^2 can be obtained. This result seems to be the best one obtained so far because it allows to reduce of about 60,000 times the occupied area with respect to a conventional IFOG with a footprint of 100 cm^2.

In this paper we identify a new solution of a frequency sensitive optical resonant gyroscope formed by three evanescently coupled ring resonators having different ring radius and coupling coefficient, which we call Resonant Micro Optical Gyroscope (RMOG), with the aim of demonstrating the feasibility of using frequency sensitive rather than phase sensitive devices.

Preliminary results of this study, together with an explanation of the difference in the operating principle of the proposed configuration with respect to a conventional CROW are reported in [21]. In particular, the resonant cavity has been designed and optimized to serve as the sensing element of an RMOG, which is a frequency sensitive gyroscope conceptually different from the CROW gyro. In the proposed TRR we have observed that when the coupled rings have different sizes and the inter-ring coupling coefficients are lower than ring-bus coupling coefficients, the Sagnac resonance wavelength difference due to the rotation is significantly magnified with respect to that of a single ring resonator occupying the same area. This result allows a strong reduction of the TRR footprint with respect to the SRR having the same scale factor. Another interesting feature of the TRR is relevant to the quality factor, evaluated as the ratio between the operative wavelength and the Full Width at Half Maximum (FWHM), which is as high as 10^6.

2 TRIPLE RING RESONATOR CONFIGURATION

We have investigated the resonant configuration shown in Figure 1, consisting of an optical cavity formed by three laterally coupled rings r1, r2 and r3 (with radius R_1, R_2, and R_3, respectively) and two straight bus waveguides. The device is excited via one straight waveguide by two counter-propagating light beams (the input field amplitudes are E_{i1} and E_{i2}), which are extracted from the other straight bus waveguide (the output field amplitudes are E_{d1} and E_{d2}).

As the resonant structure is reciprocal, the two counter-propagating beams exhibit the same optical path when the structure is at rest and, thus, $E_{d1}/E_{i1} = E_{d2}/E_{i2}$. A potential coupling between E_{i1} and E_{i2}, due to any perturbations within the structure, may lead to $E_{d1}/E_{i1} \neq E_{d2}/E_{i2}$. It can be avoided by adopting a frequency sensitive read-out technique which includes two frequency shifters for decoupling the optical frequencies of E_{i1} and E_{i2}.

At rest, the counter-propagating modes excited by E_{i1} and E_{i2} resonate at the same frequency, while, when the cavity rotates, a difference $\Delta\nu$ between the resonant frequencies is generated between the two modes. According to the IEEE standards for inertial sensor terminology [22], the scale factor SF of the gyroscope including a resonator is defined as the ratio $|\Delta\nu/\Omega|$ (where Ω is the angular velocity).

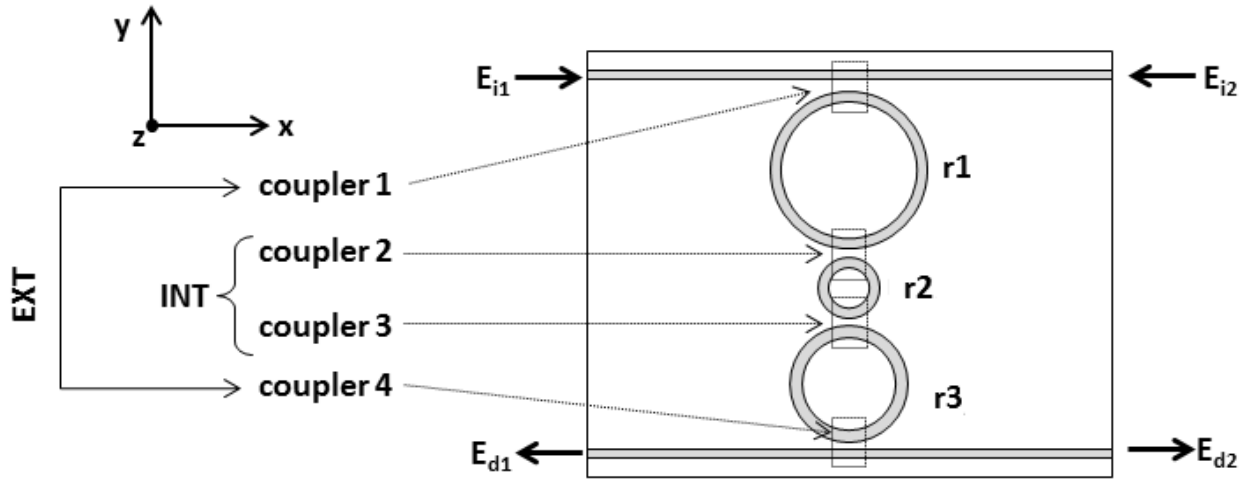

FIG. 1 Configuration of the triple ring resonator.

3 NUMERICAL RESULTS

In this section we demonstrate the enhancement of the scale factor achievable using the TRR instead of the SRR in a RMOG. Two counter propagating beams are again considered for the device operation.

In our calculations we have assumed channel waveguides made by a 6 μm × 6 μm Ge doped silica core embedded in a silica matrix on a silicon substrate. The operating wavelength is λ_0 =1.55 μm (frequency f = 193 THz), where the waveguides support the TE0 fundamental mode with effective index n_{eff} = 1.457 and propagation loss α = 0.01 dB/cm [23]. The conclusions reported here are still valid for any other fabrication technology allowing a propagating loss < 0.02 dB/cm. Although complex coupling coefficients should be considered, we have assumed real values for the coupling coefficients to simplify the calculations without losing the validity of the results we have achieved.

It is well known [1] that, in a frequency sensitive gyroscope based on a SRR, the SF can be evaluated in a simple form through the ratio between the ring diameter and the operating wavelength, SF = 2R/λ. In other words, the scale factor only depends on the ring radius, R, affecting the sensor footprint, which can be approximated to a squared area 2R×2R.

3.1 TRR spectral response

The SF in the TRR sensor can only be derived by numerically evaluating Δν. In order to achieve this goal, we calculated the spectral response of the TRR by exploiting the Masons gain rule [24], that we have modified to take into account the rotation, although other alternative approaches for the spectral response computation, such as the transfer matrix method, lead to the same results reported in this sub-section.

Once evaluated the spectral response we have derived the spectral position of the dropped resonance peak when the system is at rest. By considering the phase perturbation in each ring resonator due to the Sagnac effect, when the system is rotated by Ω, we evaluated the position of the new resonant peaks associated with the two counter propagating modes.

The phase shifts experienced by the optical beam propagating within the rings r1, r2, r3 depend on the angular velocity and, using the Z-transform formalism as in Ref. [24], we have obtained:

$$z_1^{-1} = \exp\left[-j\frac{\omega\, 2\pi R_1 n_{eff}}{c \mp R_1\Omega/n_{eff}}\right],$$
$$z_2^{-1} = \exp\left[-j\frac{\omega\, 2\pi R_2 n_{eff}}{c \pm R_2\Omega/n_{eff}}\right],$$
$$z_3^{-1} = \exp\left[-j\frac{\omega\, 2\pi R_3 n_{eff}}{c \mp R_3\Omega/n_{eff}}\right] \quad (1)$$

where j is the imaginary unit, ω is the angular frequency, and c is the speed of light in the vacuum. The term $c \pm R_i\Omega/n_{eff}$ ($i = 1,2,3$) in Eqs. (1) includes the sign '+' for the beam counter-rotating with Ω, while the sign '-' for a co-rotating beam.

The phase contributions in Eqs. (1) have been derived following the rotation kinematics treatment reported in [24]. In particular, Eqs. (1) have been obtained by considering that the phase difference, due to the Sagnac effect between the two counter propagating optical waves (CCW, counter-clockwise and CW, clockwise) in a circular path of radius R [25] is equal to:

$$\Delta\Phi = \Phi^{CCW} - \Phi^{CW} = \frac{4\pi^2 R}{c}(SF)\Omega \quad (2)$$

when a clockwise rotation is assumed. By using Eqs. (1), the phase shifts due to the Sagnac effect between two counter-propagating waves for the i-th ring result can be derived:

$$\Delta\Phi_{zi} = \Phi_{zi}^{CCW} - \Phi_{zi}^{CW} = \frac{\omega 2\pi R_i n_{eff}}{c + R_i\Omega/n_{eff}} - \frac{\omega 2\pi R_i n_{eff}}{c - R_i\Omega/n_{eff}}$$
$$\approx \frac{4\pi^2 R_i}{c}(SF_i)\Omega \quad (3)$$

where SF_i is the scale factor of the i-th ring, defined as above. The phase contributions Φ_{zi}^{CCW} and Φ_{zi}^{CW} affect the overall spectral behavior of the TRR under rotation in a way which is unpredictable by an analytical approach.

The spectral response T of the TRR, following the mathematical procedure described in [24], has been derived by calculating the determinant Δ of the flow graph related to the optical path of the waves in the resonating structure, and the transfer function Y taking into account the amplitude and phase contributions in the open path connecting the device input to the output.

The Mason's gain rule states that $T = |Y/\Delta|^2$ and so the spectral response is given by:

$$T = \left| \sqrt{\eta_1\eta_2\eta_3\eta_4\gamma_1\gamma_2\gamma_3}\sqrt{z_1^{-1}z_2^{-1}z_3^{-1}} \cdot \left(1 - \gamma_1\tau_1\tau_2 z_1^{-1} - \gamma_2\tau_2\tau_3 z_2^{-1} - \gamma_3\tau_3\tau_4 z_3^{-1} + \gamma_1\gamma_2\tau_1\tau_3 z_1^{-1}z_2^{-1} + \gamma_2\gamma_3\tau_2\tau_4 z_2^{-1}z_3^{-1} + \gamma_3\gamma_1\tau_1\tau_2\tau_3\tau_4 z_1^{-1}z_3^{-1} - \gamma_1\gamma_2\gamma_3\tau_1\tau_4 z_1^{-1}z_2^{-1}z_3^{-1}\right)^{-1} \right| \quad (4)$$

where η_1 and η_4 are the external power coupling coefficients between the rings and the straight bus waveguides (assumed to be equal and denoted η_{EXT} in the following) while η_2 and η_3 are the inter-ring coupling coefficients (assumed to be equal and denoted η_{INT} in the following). τ_h (h = 1,..,4) is the transmission coefficient of the h-coupler and is equal to $\tau_h = (1\text{-}\eta_h)^{1/2}$. The γ coefficients take into account the attenuation suffered by the optical beam in the rings.

The cavity was designed assuming $R_2 << (R_1, R_3)$ and R_3 slightly less than R_1, in order to exploit Vernier effect advantages [26]. R_2 should be > 0.35 cm for the bending loss in the central ring to be negligible. We optimized the ratios between the radii in order to increase the free spectral range up to 0.36 nm, at the wavelength λ_0 = 1.55 μm. The rings have been designed as resonating at that wavelength. Therefore the following conditions have to be satisfied:

$$R_1 = q_1\frac{\lambda_0}{2\pi n_{eff}}, \quad R_2 = q_2\frac{\lambda_0}{2\pi n_{eff}}, \quad R_3 = q_3\frac{\lambda_0}{2\pi n_{eff}} \quad (5)$$

and where q_1, q_2, and q_3 are the resonance orders (integer numbers) relevant to each ring.

Since λ_0/n_{eff} = 50/47 μm, we have chosen q_1, q_2, and q_3 as multiple of 47 in order to have the ring lengths (denoted as L_1, L_2, L_3, respectively) as integer quantities. Then, by assuming q_1 = 77832, q_2 = 21620 and q_3 = 73508, we obtain L_1 = 82800 μm, $L_2 = (5/18)L_1$, and $L_3 = (17/18)L_1$ and R_1 = 1.3178 cm, $R_2 = (5/18)R_1$, and $R_3 = (17/18)R_1$. With this geometry, the device has a footprint of about 15 cm^2.

For $\eta_{EXT} = \eta_{INT}$, the TRR sensor does not show any improvement of the scale factor with respect to a single ring with a radius R_1. Therefore, in this case we have $SF_T = 2\,R_1/\lambda_0$. This behavior is also confirmed when the rings of the TRR have the same size. Also for $\eta_{EXT} < \eta_{INT}$, SF_T is very close to $2\,R_1/\lambda_0$. When $\eta_{EXT} \leq \eta_{INT}$ the TRR exhibits a transmission spectrum with several lateral fringes due to Fabry-Perot-like interference between the two ends of the resonating structure [27]. In this case the resonance peak has a Lorentzian shape (the same shape of the SRR spectral response) and thus the TRR behaviour under rotation is very similar to that one of a SRR, with no enhancement of the scale factor.

Depending on the values of η_{EXT} and η_{INT}, an enhancement of the scale factor can be obtained when $\eta_{EXT} > \eta_{INT}$. In fact, the condition $\eta_{EXT} > \eta_{INT}$ allows the lateral peaks of the spectral response to be rejected by keeping constant the pass band width of the overall structure, as experimentally proved in [29] for two coupled rings. The spectral response of the TRR is in this way forced to assume a shape, which is not Lorentzian and more sensitive to the resonant frequency shift due to rotation with respect to the SRR case.

In the TRR, for $\eta_{EXT} > \eta_{INT}$, the rotation induces a change in the shape of the transmission curve, because the interaction of the optical waves within the multi-path structure is influenced by new phase contributions due to rotation. The above mentioned interaction and the resultant transmission shape are controlled through the fraction of power flowing from one ring to another (η_{INT}) or to a straight waveguide (η_{EXT}). Therefore, the rotation induced frequency shift observed in the spectrum response is influenced by both internal and external coupling coefficients. In the next subsection the TRR spectrum response, optimized in relation with η_{INT} and η_{EXT} values (η_{INT} = 0.011, η_{EXT} = 0.381) in order to obtain a scale factor magnification, is described.

3.2 TRR scale factor

On the basis of our numerical simulations, by evaluating SF_T as previously described, we concluded that the scale factor of the TRR can be written as:

$$SF_T = K\,SF_s \quad (6)$$

where K is the scale factor enhancement obtainable in the TRR when $\eta_{EXT} > \eta_{INT}$ and the rings have different size. K has been evaluated numerically, as clarified in the previous subsection, and it represents the ratio between SF_T and SF_S, which is the scale factor of a frequency sensitive gyro based on a single ring having the same area of the TRR. The footprint of the TRR can be approximated to a rectangle of size $2R_1 \times L_{tot} = (80/9)R_1^2$, where $L_{tot} = 2R_1 + (5/9)R_1 + (17/9)R_1$. Thus, the occupied area is equal to $(80/9)R_1^2$. In order to have the same footprint of the triple ring, a single ring is required to have a radius equal to $(R_1/2)\times(80/9)^{1/2}$.

Since SF_T can also be negative, K can be either positive or negative, depending on the sense of rotation. The dependence of the enhancement factor K on the ratio η_{EXT}/η_{INT} is shown in Figure 2, for η_{INT} = 0.01, 0.05, 0.10, 0.20, 0.60. In all curves we can observe that, for low values of the ratio η_{EXT}/η_{INT}, K increases as the ratio increases. After reaching the maximum value, K quickly becomes negative when the ratio η_{EXT}/η_{INT} increases again. The K factor increases as the ratio η_{EXT}/η_{INT} increases after achieving the minimum value. In principle, we can utilize both the maximum and the minimum of K to obtain $|K| > 1$. The five curves plotted in Figure 2 exhibit a maximum ranging from 1.88 (for η_{INT} = 0.01) to about 3 (for η_{INT} = 0.20). Because of the high flexibility of the TRR, allowing the condition $|K| > 1$ to be obtained for a wide range of η_{EXT} and η_{INT} values, the most appropriate value of η_{INT} to be utilized in the optimized design can be selected by considering other sensor parameters, e.g. the resonator quality factor Q. Since Q can be maximized by selecting low values of η_{INT}, in our design, we

put η_{INT} = 0.01 to allow a quality factor of the order of 10^6, as highlighted later in this subsection.

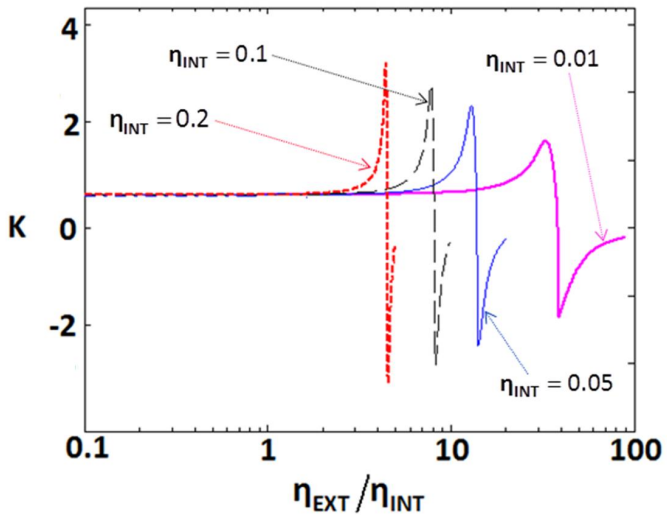

FIG. 2 K vs. η_{EXT}/η_{INT} for η_{INT} = 0.01, 0.05, 0.10, and 0.20. for a triple ring resonant gyroscope with R_1 = 1.3178 cm, R_2 = (5/18)R_1, R_3 = (17/18)R_1.

In particular, as an example, for η_{EXT} = 0.311 and η_{INT} = 0.011 (η_{EXT} / η_{INT} = 28.27), SF_T becomes about 1.50 times SF_S, while for η_{EXT} = 0.381 and η_{INT} = 0.011 (η_{EXT}/η_{INT} = 34.65) SF_T improved up to 1.88 times SF_S (see Figure 2). In Figure 3 the frequency shift $|\Delta\nu|$ is reported as a function of Ω at different combinations of values of (η_{EXT}, η_{INT}). The angular rate range (0–100 rad/s) reported in Figure 3 has been chosen in order to consider a linear range of angular velocity values of practical interest for all application domains. The results in Figure 3 demonstrate the very good linearity of the sensor.

For η_{EXT} and η_{INT} values corresponding to $SF_T = 1.50 \cdot SF_S$ and $SF_T = 1.88 \cdot SF_S$ the TRR quality factor, evaluated as the ratio between the operating wavelength and the linewidth of dropped resonance, is of the order of 10^6. The single ring resonator having the same footprint of the TRR has an optimized Q-factor of the same order of magnitude 10^6. The spectral response of TRR with η_{EXT} = 0.3811 and η_{INT} = 0.011 is reported in Figure 4.

In this figure we can observe that the spectral response of the TRR does not show any resonance lateral peaks, that can be observed together with a central peak of Lorentzian shape

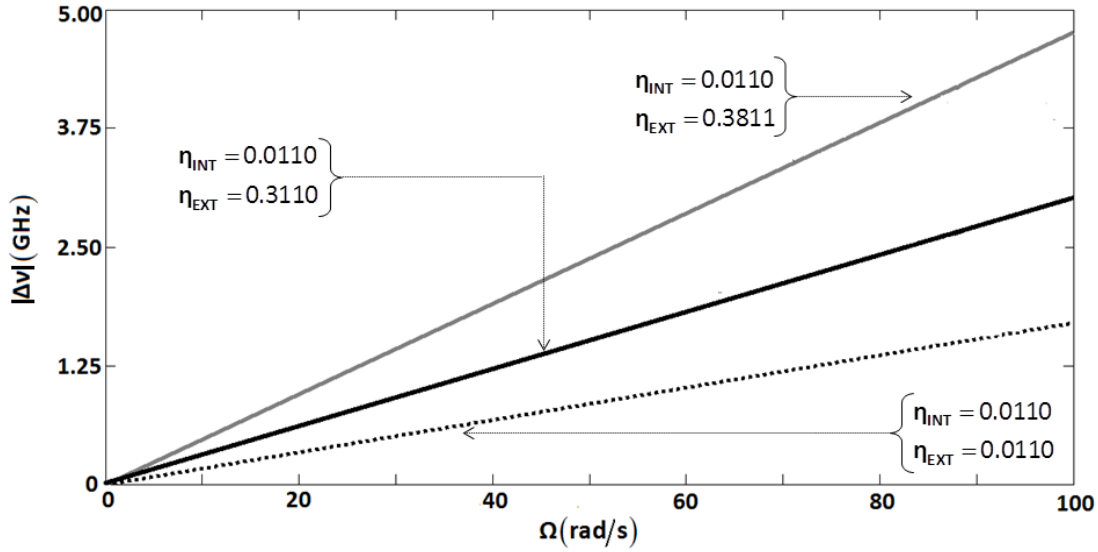

FIG. 3 Dependence of the resonance frequency difference $|\Delta\nu|$ on the angular velocity Ω for the TRR as in Figure 2 with R_1 = 1.3178 cm, R_2 = (5/18)R_1, R_3 = (17/18)R_1.

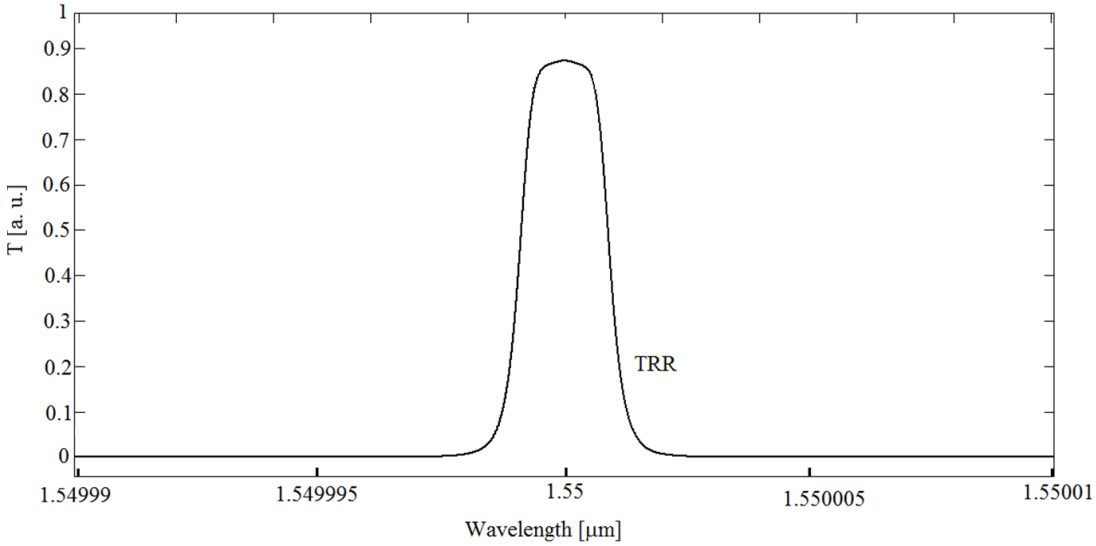

FIG. 4 Spectral response of the TRR as in Figure 2 with R_1 = 1.3178 cm, η_{EXT} = 0.381 and η_{INT} = 0.011.

when $\eta_{EXT} = \eta_{EXT}$ [29]. Just one peak with a non Lorentzian shape is shown in Figure 4, from which we have calculated a Q factor of $1{\cdot}10^6$. The free spectral range of the TRR is 18 times that one of the SRR, as expected due to the Vernier effect [24], and, in turn, the finesse of the resonant structure is enhanced of the same value. The finesse and the free spectral range of the TRR can be exploited in order to improve spectral selectivity of TRR-based sensors. On the other hand, we would just to remind that the Q factor is a crucial parameter to enhance the resolution of a resonant optical gyroscope.

4 CONCLUSION

In this paper we have studied a resonant cavity, formed by three ring resonators having different ring radii and coupling ratios, to be used as sensing element of a frequency sensitive resonant optical gyroscope. Being frequency sensitive, the proposed device shows a physical behavior different from the CROW gyros. In fact, instead of detecting the power variation associated to the Sagnac effect, as in CROW gyros, it allows to derive the angular velocity through a spectrometric technique, which consists in the discrimination of the shift between the resonant frequencies of the two counter-propagating modes.

By optimizing the values of the ring radius and inter-ring and ring-bus coupling coefficients we have demonstrated that the scale factor, related to the variation of the resonance frequencies of two counter-propagating beams, in a triple ring resonator is higher than that of a single ring resonator occupying the same footprint.

While in a single ring resonator the scale factor enhancement can be achieved only by increasing the sensor footprint, which means tighter requirements on the uniformity of the fabrication process, in the proposed triple ring resonator we have demonstrated that the increase of the scale factor can be obtained without increasing the sensor footprint. This result is a crucial advantage of the triple ring resonator with respect to the single ring resonator not only in terms of compactness and weight, but also in terms of fabrication requirements.

For the proposed sensor the scale factor magnification allows the reduction of the sensor footprint of about 1.88 times with respect to a single ring device, with a Q factor as high as 10^6.

The results we have obtained in this research may lead to a very promising technique for manufacturing miniaturized and high-performance integrated optics sensors to be used mainly in aerospace applications.

References

[1] C. Ciminelli, F. Dell'Olio, C. E. Campanella, and M. N. Armenise, "Photonic technologies for angular velocity sensing," Adv. Opt. Photon. **2**, 370–404 (2010).

[2] M. N. Armenise, C. Ciminelli, F. Dell'Olio, V. M. N. Passaro, *Advances in Gyroscope Technologies* (Springer-Verlag, 2010).

[3] O. Kenji, "Semiconductor ring laser gyro," Japanese patent # JP 60,148,185, filed 1984, issued 1985.

[4] M. Armenise, P. J. R. Laybourn, "Design and Simulation of a Ring Laser for Miniaturised Gyroscopes," Proc. SPIE **3464**, 81–90 (1998).

[5] M. N. Armenise, M. Armenise, V. M. N. Passaro, and F. De Leonardis, "Integrated optical angular velocity sensor," European patent # EP1219926, filed 2000, issued 2010.

[6] M. Osiński, H. Cao, C. Liu, and P. G. Eliseev, "Monolithically integrated twin ring diode lasers for rotation sensing applications," J. Cryst. Growth **288**, 144–147 (2006).

[7] W. Lawrence, "Thin film laser gyro," US patent # 4,326,803, filed 1979, issued 1982.

[8] K. Suzuki, K. Takiguchi, and K. Hotate, "Monolithically integrated resonator microoptic gyro on silica planar lightwave circuit," J. Lightwave Technol. **18**, 66–72 (2000).

[9] C. Ciminelli, F. Peluso, and M. N. Armenise, "A new integrated optical angular velocity sensor," Proc. SPIE **5728**, 93–100 (2005).

[10] C. Ciminelli, C. E. Campanella, and M. N. Armenise, "Optimized Design of Integrated Optical Angular Velocity Sensors Based on a Passive Ring Resonator," J. Lightwave Technol. **27**, 2658–2666 (2009).

[11] H. Mao, H. Ma, and Z. Jin, "Polarization maintaining silica waveguide resonator optic gyro using double phase modulation technique," Opt. Express **19**, 4632–4643 (2011).

[12] C. Ciminelli, F. Dell'Olio, M. N. Armenise, F. M. Soares, and W. Passenberg, "High performance InP ring resonator for new generation monolithically integrated optical gyroscopes," Opt. Express **21**, 556–564 (2013).

[13] C. Ciminelli, F. Dell'Olio, C. E. Campanella, and M. N. Armenise, "Numerical and experimental investigation of an optical high-Q spiral resonator gyroscope," in *Proceedings to the 14th International Conference on Transparent Optical Networks (ICTON)*, 1–4 (IEEE Photonics Society, Coventry, UK, 2012).

[14] C. Ciminelli, F. Dell'Olio, and M. N. Armenise, "High-Q Spiral Resonator for Optical Gyroscope Applications: Numerical and Experimental Investigation," IEEE Photonics J. **4**, 1844–1854 (2012).

[15] J. Schuer, and A. Yariv, "Sagnac Effect in Coupled-Resonator Slow-Light Waveguide Structures," Phys. Rev. Lett. **96**, 05390 (2006).

[16] M. Terrel, M. J. F. Digonnet, and S. Fan, "Performance comparison of slow-light coupled-resonator optical gyroscopes," Laser Photonics Rev. **3**, 452–464 (2009).

[17] B. Z. Steinberg, J. Scheuer, and A. Boag, "Rotation Induced Super Structure in Slow-Light Waveguides with Mode Degeneracy," J. Opt. Soc. Am. B **24**, 1216–1224 (2007).

[18] R. Novitski, B. Z. Steinberg, and J. Scheuer, "Losses in rotating degenerate cavities and a coupled-resonator optical-waveguide rotation sensor," Phys. Rev. A **85**, 023813 (2012).

[19] J. R. E. Toland, Z. A. Kaston, C. Sorrentino, and C. P. Search, "Chirped area coupled resonator optical waveguide gyroscope," Opt. Lett. **36**, 1221–1223 (2011).

[20] C. Sorrentino, J. R. E. Toland, and C. P. Search, "Ultra-sensitive chip scale Sagnac gyroscope based on periodically modulated coupling of a coupled resonator optical waveguide," Opt. Express **20**, 354–363 (2012).

[21] C. Ciminelli, C. E. Campanella, F. Dell'Olio, C. M. Campanella, and M. N. Armenise, "Multiple ring resonators in optical gyroscope," in *Proceedings to the 14th International Conference on Transparent Optical Networks (ICTON)*, 1–4 (IEEE Photonics Society, Coventry, UK, 2012).

[22] IEEE Standard for Inertial Sensor Terminology, IEEE Std 528-2001 (2001).

[23] R. Adar, M. R. Serbin, and V. Mizrahi, "Less than 1 dB per meter propagation loss of silica waveguides measured using a ring resonator," J. Lightwave Technol. **12**, 1369–1372 (1994).

[24] S. Mandal, K. Dasgupta, T. K. Basak, and S. K. Ghosh, "A generalized approach for modeling and analysis of ring-resonator performance as optical filter," Opt. Commun. **264**, 97–104 (2006).

[25] S. Ezekiel, and H. J. Arditty, *Fiber-Optic Rotation Sensors and Related Technologies* (Springer, New York, 1982).

[26] G. Barbarossa, M. N. Armenise, and A. M. Matteo, "Triple-coupler ring-based optical guided-wave resonator," Electron. Lett. **30**, 131–133 (1994).

[27] S. Olivier, C. Smith, M. Rattier, H. Benisty, C. Weisbuch, T. Krauss, R. Houdré, and U. Oesterlé, "Miniband transmission in a photonic crystal coupled-resonator optical waveguide," Opt. Lett. **26**, 1019–1021 (2001).

[28] M. Sumetsky, and B. Eggleton, "Modeling and optimization of complex photonic resonant cavity circuits," Opt. Express **11**, 381–391 (2003).

[29] R. Boeck, N. A. F. Jaeger, N. Rouger, and L. Chrostowski, "Series-coupled silicon racetrack resonators and the Vernier effect: theory and measurement," Opt. Express **18**, 25151–25157 (2010).